CHARACTERISATION OF A MOBILE JAW CRUSHER FOR SMALL SCALE MINING AND CONSTRUCTION INDUSTRY

A. J. M. Itika

Department of Mining and Mineral Processing, University of Dar es Salaam,
P. O. Box 35131, Dar es Salaam, Tanzania,
E-mail: aitika@udsm.ac.tz

ABSTRACT

A small jaw crusher with a crushing capacity of 1 ton per hour has been developed for use in the small scale mining and construction industry. A 3.68 kW air cooled diesel engine was installed to power the crusher. Laboratory and field test were conducted using limestone as feed material at different operating parameters. The analysis of the product from the crusher showed that at a constant jaw gap, coarser products were obtained when the rotary speed was varied from 220 rpm to 300 rpm. With a jaw gap of 25 mm, a higher cumulative undersize fraction was obtained at particle size 25 mm. In contrast, at a jaw gap of 15 mm, higher cumulative undersize fraction was obtained at particle size 15 mm. With a feed size 80% passing 60 mm, a finer product was obtained as compared to a feed 80% passing 120 mm. The throughput of the machine increased from 0.4 ton/hr to 0.7 ton/hr when the speed was increased from 220 rpm to 300 rpm. It was found that it is possible to select a combination of operating parameters to achieve a particular goal of operation.

(***Key words***: crushing, crusher, jaw crusher, size reduction, comminution, limestone crushing, small scale crushing machine)

INTRODUCTION

Crushing is the initial essential unit operation in mineral processing that helps reducing the size of materials to manageable sizes for further processing. Crushing is usually a dry process that is performed in several stages, with small *reduction ratios* ranging from three to six in each stage. The reduction ratio of a crushing stage can be defined as the ratio of maximum particle size entering to maximum particle size leaving the crusher. From the initial to the final stage particles may be reduced in size from over 1500 mm to 5-25 mm depending on the specific process requirements.

At the microscopic level, two conditions are known to be necessary for a particle to break. These are the strength and the energy conditions.

➢ The strength condition demands that at the breakfront of the particle the forces binding its elementary components (molecular strength) must be exceeded by the applied stresses *Schoenert [1991], Rumpf [1959]*. However, in reality, it is found that the tensile stress at the breakfront is smaller by a factor of two to three power ten than the molecular strength of the particle at the breaking point. This has been explained by the notch effect caused by the presence of cracks and defects in the particle. This condition postulates the presence of a minimum crack whose size must increase to explain a further reduction in the yield stress of the particle compared to its molecular strength.

➢ At the same time the energy condition requires that for a differential crack propagation, the elastic energy set free or released by the propagating breakage must equal or exceed the boundary surface energy to be built up. *Griffith [1921]* made this assumption and came up with the inequality

$$-\frac{\partial U_a}{\partial l} \geq \frac{\partial S_o}{\partial l} \qquad (1)$$

where U_a is the energy of deformation and S_o is the boundary surface energy.

At a particular crack length known as Griffith length, the system is balanced. At higher crack

length $I > I_{griff}$ the elastic energy term $-\partial U_a/\partial l$ grows and the crack propagates further.

Mechanisms of Stressing

Rumpf [1959] has defined three different mechanisms of stressing a particle. These are shown in Figure 1. A particle can be stressed between two surfaces, a process usually termed compression (Fig. 1a). In this category the shape of the stressing surface is immaterial allowing for consideration of even two sharp surfaces.
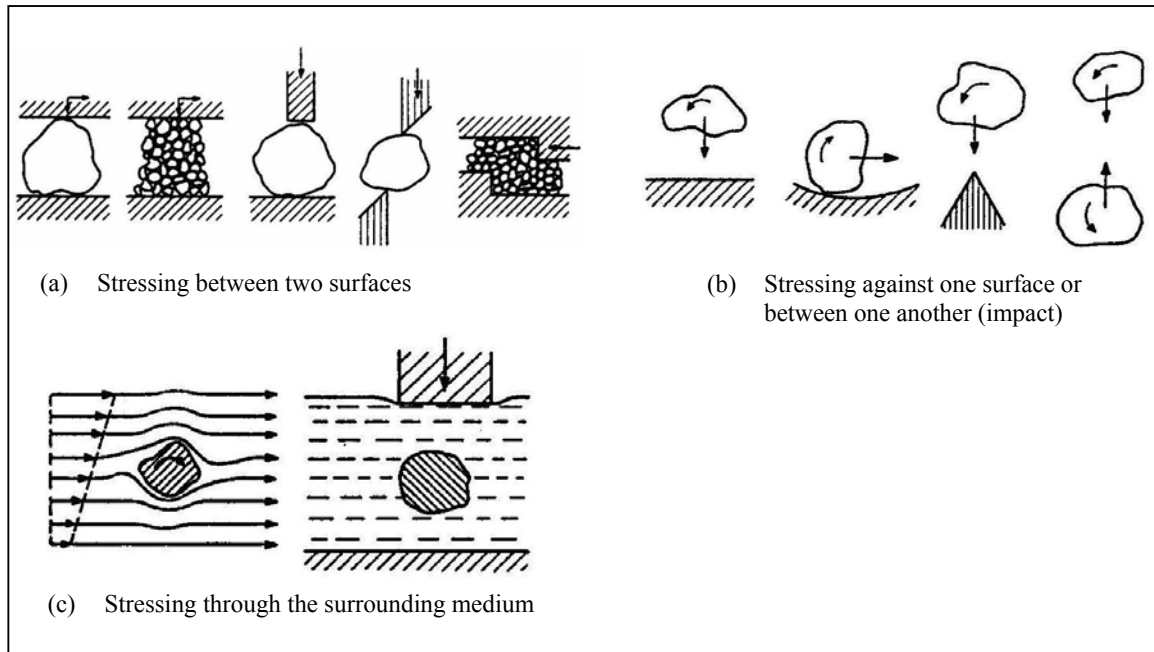

(a) Stressing between two surfaces

(b) Stressing against one surface or between one another (impact)

(c) Stressing through the surrounding medium

**Figure 2:** Stressing mechanisms of a particle *(Rumpf 1959)*

The particles can be stressed singly or collectively. Further, the particle can be stressed against a surface whereby either the particle or the surface is in motion (Figure **2**b). Alternatively, the particle can strike against another particle in a similar way. In this category, attrition of the particle usually accompanies the impact event especially because the particle is free to rotate.

The third stressing mechanism occurs when the particle finds itself surrounded by a medium (Figure **2**c). The stresses are induced due to relative motion of the fluid body or due to application of pressure waves on the fluid surface. This type of stressing can be important only in wet grinding.

Crushing by Machines
Over the years a number of machines have been developed that are applied for crushing materials to different sizes. The machines apply different stressing principles or a combination of them to effect the crushing. These include shear stress, compressive stress, bending stress, tensile stress, friction, impact, attrition etc. Among the machines that are applied for crushing are jaw crushers and cone crushers.

The energy required for size reduction in a machine is many times that actually required for the production of a new surface. The reason for this is that a lot of energy is being wasted in the friction of particles, in the deformation of the particles, as kinetic energy of the broken pieces, wear of the surfaces, sound and heat generation.
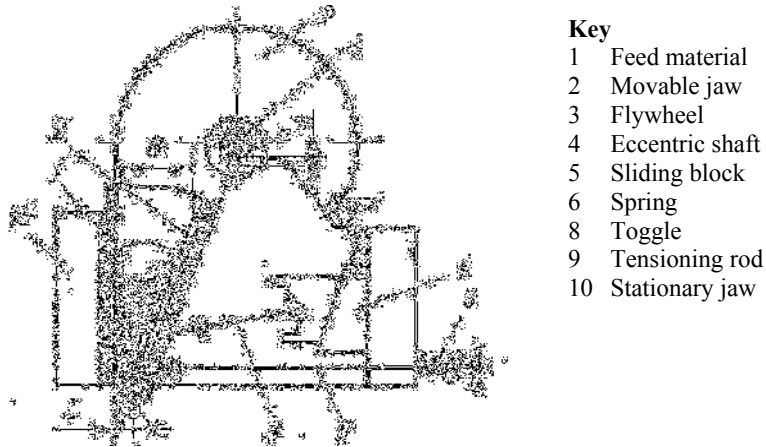
Key
1 Feed material
2 Movable jaw
3 Flywheel
4 Eccentric shaft
5 Sliding block
6 Spring
8 Toggle
9 Tensioning rod
10 Stationary jaw

Figure 3: The jaw crusher showing the main parts

The jaw crusher consists basically of two jaws one movable and the other stationary. The movable jaw is pivoted at the lower end and is suspended on an eccentric shaft at the top. The jaw is slanted at an angle of about 24° *[Hoeffl 1986]*.

The Design Calculations for the Jaw Crusher
The angle of inclination
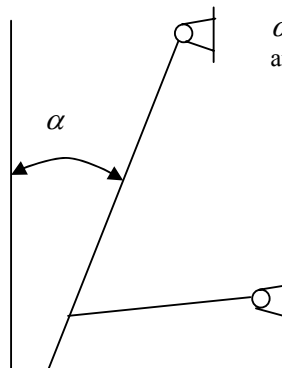
α is the angle between the stationary and movable jaws

Figure 4: The angle of inclination of the jaw crusher

The maximum angle of inclination between the stationary and movable jaw can be estimated from:

$$tan\frac{\alpha}{2} \leq \mu \qquad (2)$$

where μ is the coefficient of friction

The eccentric motion of the shaft causes a helical motion of the movable jaw that continuously applies pressure at the feed material that is stepwise allowed to drop through the crushing chamber under gravity as it breaks. The bottom gap of the crusher "t" determines the size of the product. The gap can be adjusted to suit the requirements of the user.

If μ is assumed to be 0.3 then the angle α becomes about 33°. For design purposes a smaller value would be used.

The critical number of revolution of the shaft
The critical number of revolution of the shaft may be calculated from the relation:

$$n_{Gr} = \frac{1}{2}\sqrt{g\,tan\frac{\alpha}{2h}} \qquad (3)$$

where g is the acceleration due to gravity, h is the throw of the movable jaw (the bottom displacement of the jaw) and α is the angle of inclination of the movable jaw to the stationary jaw. In practice, the number of revolution of the drive shaft lies between 10 and 15% of the critical speed.

The throughput

An assumption is made that the crushed material moves in the crushing chamber like a prism. The throughput is therefore calculated from:

$$\dot{V} = Vn\varphi \qquad (4)$$

where V is the volume of the falling prism, n is the number of revolutions of the drive shaft and φ is the voidage of the broken materials in the falling prism (0.3-0.5)

The volume of the falling prism can be calculated from:

$$V = \frac{(2s+h)bh}{2\,tan\,\alpha} \qquad (5)$$

Combining the two equations the throughput can be found from *[Hoeffl 1986]*:

$$\dot{V} = \frac{\varphi n(s+h/2)hb}{tan\,\alpha} \; m^3/s \qquad (6)$$

To get the mass throughput one simply multiplies the above equation with the bulk density of the broken materials.

EXPERIMENTAL WORK

The crusher was developed and mounted on a special three wheeler bicycle as shown in Figure 5. The crusher was powered by a 3.5 HP diesel engine.
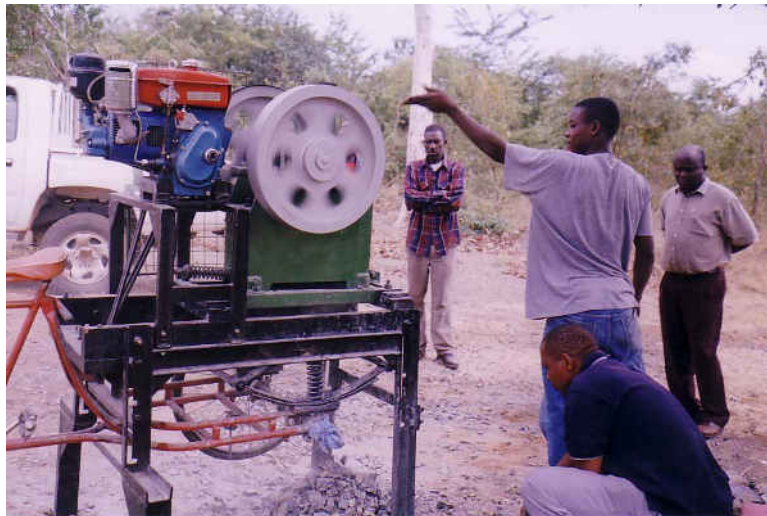

Figure 5: The small scale jaw crusher being tested

Various parameters including discharge gap, rotational speed of the drive shaft, rate of feed, feed size and nature of feed material were investigated on the crusher. One parameter was varied as the others were kept constant. Speed tests were conducted using a variable speed motor that was coupled to a gear box. Rotational speeds of the machine were monitored using tachometer verified with a stroboscope. The product size was analyzed using standard sieves. Each parameter was investigated at least three times to check the consistency and accuracy of the results obtained. Care was taken to ensure no product contamination from one experiment to the other.

DISCUSSION OF RESULTS

The Influence of the Number of Revolution on the Product

Tests were conducted to investigate the influence of the number of revolution of the crusher at two different jaw gaps. Pre-crushed limestone of average size 12 cm obtained from Mtongani Quarry was used as feed material. A jaw gap of 15 mm was used in this set of experiments. Figure 6 shows the cumulative undersize fraction at revolution speeds between 220 rpm and 300 rpm. From the graphs it can be seen that generally finer product was obtained at lower speeds of the machine. However, deviations from this trend have been observed at product sizes below 12.5 mm. In that size range, finer product was obtained at a

revolution speed of 260 rpm as compared to the other speeds. Looking at the general trend at the revolution speed of 220 rpm, the cumulative fraction of 43% at the product size of 12.5 mm is an outlier. At the highest revolution speed of 300 rpm coarser product is obtained throughout the considered size range.

At the revolution speed of 220 rpm, 80% of the product was finer than 20 mm. For the other revolution speeds of 240 rpm, 260 rpm, and 300 rpm, 80% of the products were finer than 22 mm, 23 mm and 25 mm respectively (Figure 6). Considering that the jaw gap was 15 mm, it would be desirable to attain higher percentage of the product in the lower size range of around 15 mm. Only 43 − 54% of the product is finer than 15 mm at the tested revolution speeds.
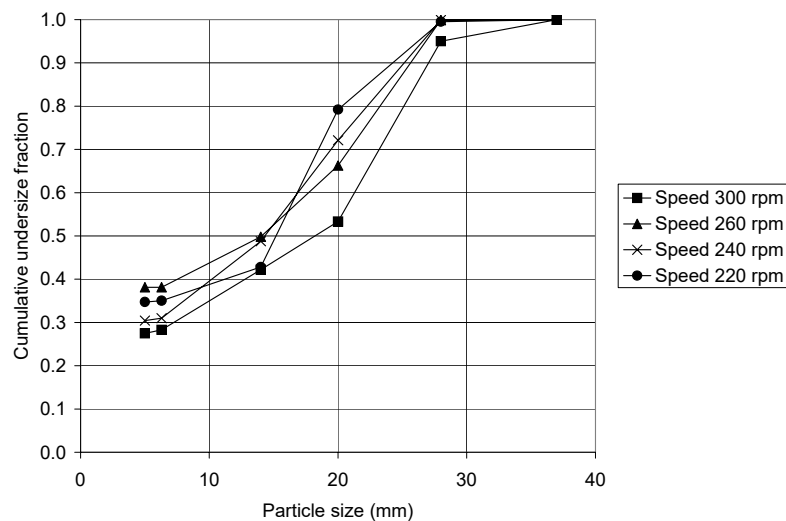

Figure 6: The influence of the number of revolution on the product at a jaw gap of 15 mm.

Similarly, results were obtained at a jaw gap of 25 mm when the revolution speed of the machine was varied between 220 rpm and 300 rpm. From Figure 7 it can be seen that finest

product was obtained at a revolution speed of 220 rpm having a mean particle size (x_{50}) of 11 mm. At this revolution speed, 80% of the product had a size smaller than 21 mm.
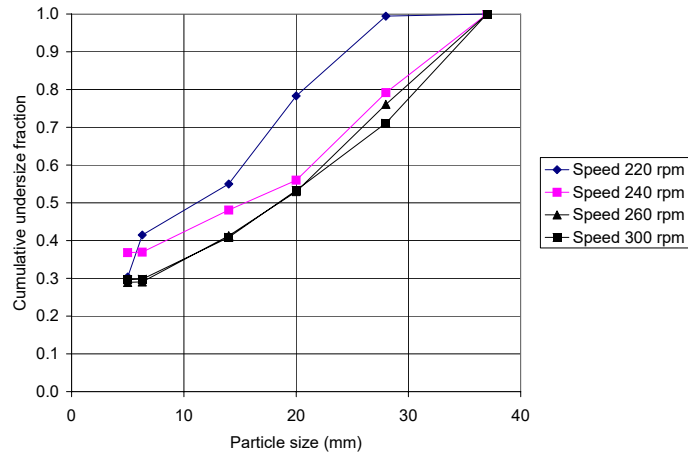
Figure 7: The influence of the number of revolution on the product at a jaw gap of 25 mm.

At this jaw gap, the size distribution of the product at a speed of 240 rpm, 260 rpm and 300 rpm are closer to each other as compared to that at a speed of 220 rpm. The mean particle sizes x_{50} of the products are respectively 15 mm, 18 mm and 18 mm. Furthermore, the 80% passing product sizes were 28 mm, 30 mm and 31 mm at the revolution speeds of 240 rpm, 260 rpm and 300 rpm respectively.

From these results, it is seen that at the revolution speed of 220 rpm, the change of jaw gap had practically no influence on the 80% passing product size. However at the other revolution speeds a marked change was observed as shown in
Table 9.

Table 9: The influence of jaw gap size and number of revolution on the product size (80% passing size)

Revolution speed	240 rpm	260 rpm	300 rpm
Jaw gap	80% passing size [mm]		
15 mm	22	23	25
25 mm	28	30	31

It is probable that at higher revolution speed the residence time of the particles is shortened resulting into coarser product. This overshadows any advantage that could have been exploited from faster stressing rate at higher speed.

The Influence of Revolution Speed on Throughput
It was observed from the experiments that the speed of the machine had an influence on the throughput.
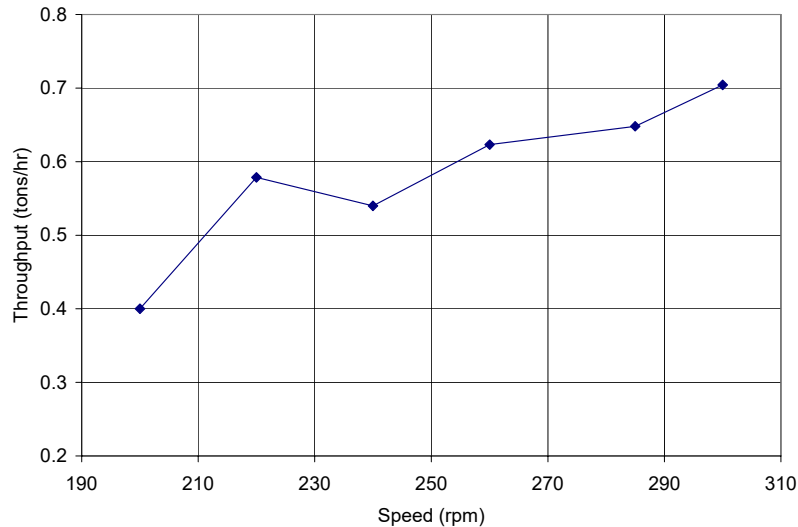
Figure 8: The dependence of the throughput on the speed at a jaw gap of 15 mm

The general trend is increased throughputs at higher speeds of the crusher. The throughput was increased from 0.4 ton/hr at a speed of 200 rpm to 0.7 ton/hr at a speed of 300 rpm. This however, has the implication that the material has less residence time in the crushing chamber and therefore the product tends to be coarser (Figure 6, Figure 7).

The Influence of Feed Size on the Product
Feed sizes of 80% finer than 60 mm, 90 mm, and 120 mm were used during the experiments. It was observed that there was insignificant

change in product size when using feed of 60 and 90 mm. However, coarser product was obtained when using feed material with size 120 mm. The size of the 80% passing product increased with increasing feed size from 28 mm at feed size of 60 mm to 30.5 mm at feed size of 120 mm. The product size variation seems to be more pronounced at the lower product size below 22 mm. 40% of the product fall in this size range. There is insignificant difference in product size when using feed of 80% passing 60 mm and 90 mm (Figure 9).
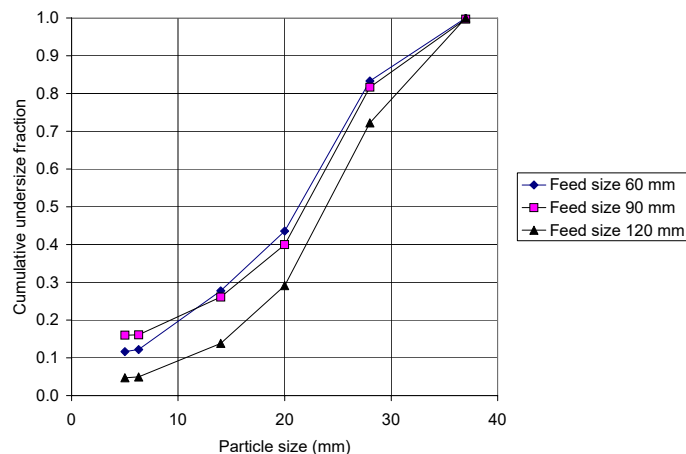

Figure 9: The influence of feed size on the product at a gap of 25 mm

The Influence of Gap Size
The conducted experiments showed that there is a clear relationship between the jaw gap and the product size obtained. Generally finer product was obtained when the jaw gap was reduced (Figure 10).
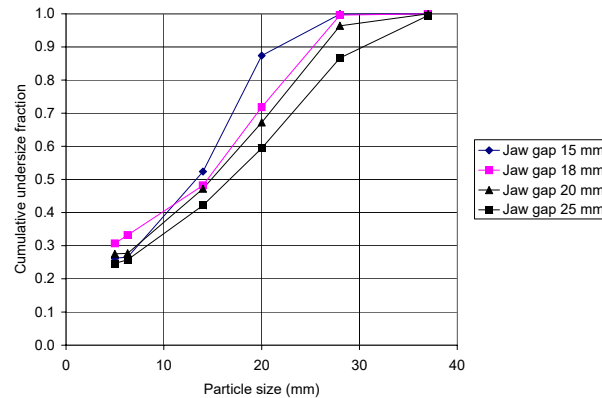

Figure 10: The variation of the product size distribution with the change in jaw gap

The product size seems to converge in the lower size range below 15 mm. The product cumulative undersize fraction, at a particle size equal to the jaw gap, increased with increasing jaw gap (Table 2)

Table 10: Product cumulative undersize fraction at particles equal to the jaw gap

S/No.	Jaw gap [mm]	Particle size [mm]	Cumulative undersize fraction
1	15	15	0.58
2	18	18	0.63
3	20	20	0.67
4	25	25	0.76

When the jaw gap of 15 mm was used, a cumulative undersize fraction of 0.58 was obtained for a particle size of 15 mm. In comparison, when the jaw gap was 25 mm, a cumulative undersize fraction of 0.76 was obtained for a particle size of 25 mm. If we retain the definition of the product size as "80% passing", then we may infer that the product size gets closer to the jaw gap with increasing jaw size.

CONCLUSION

The behaviour of the crusher varies with both operating and structural characteristics. These results have been based on limestone available in a location at Dar es Salaam. Material characteristics may have influence on the results obtained and therefore need to be considered when interpreting these results under different conditions. The behaviour of the crusher has been found to conform to general established knowledge in the area of comminution.

ACKNOWLEDGEMENT

NOMENCLATURE

Item	Description	Unit
U_a	Energy of deformation	J/m^2
V	Volume	m^3
$\dot{V}$	Throughput	m^3/s
S_o	Boundary surface energy	J/m^2
g	Acceleration due to gravity	m/s
φ	Voidage	-
I	Crack length	m

I_{griff}	Griffith length	m
α	Angle of inclination	o
μ	Coefficient of friction	Ns^2/m^4
h	The throw of the movable jaw	m
n_{Gr}	Critical number of revolution	s^{-1}

REFERENCE

Griffith, A. A., (1921): The phenomena of rupture and flow in solids", Philos. Trans. Royal Society of London, Serial A, 221, 163/98.

Hoeffl, Karl, (1986): "Zerkleinerungs- und Klassiermaschinen", Springer-Verlag, Berlin

Rumpf, H., (1959): "Beanspruchungs-theorie der Prallzerkleinerung", technische Chemie, Verfahrenstechnik und Apparatenwesen, Verlag Chemie GmbH, Weinheim, 31(1959)5 p. 323-337

Schoenert, K., (1991): "Advances in Comminution Fundamental and Impact in Technology", XVII International Mineral Processing Congress, Dresden.